


Metastasized lung cancer suppression by *Morinda citrifolia* (Noni) leaf compared to Erlotinib via anti-inflammatory, endogenous antioxidant responses and apoptotic gene activation

Swee-Ling Lim¹ · Noordin M. Mustapha² · Yong-Meng Goh² · Nurul Ain Abu Bakar¹ · Suhaila Mohamed¹ 

Received: 20 October 2015 / Accepted: 6 April 2016
© Springer Science+Business Media New York 2016

Abstract Metastasized lung and liver cancers cause over 2 million deaths annually, and are amongst the top killer cancers worldwide. *Morinda citrifolia* (Noni) leaves are traditionally consumed as vegetables in the tropics. The macro and micro effects of *M. citrifolia* (Noni) leaves on metastasized lung cancer development in vitro and in vivo were compared with the FDA-approved anti-cancer drug Erlotinib. The extract inhibited the proliferation and induced apoptosis in A549 cells ($IC_{50} = 23.47 \mu\text{g/mL}$) and mouse Lewis (LL2) lung carcinoma cells ($IC_{50} = 5.50 - \mu\text{g/mL}$) in vitro, arrested cancer cell cycle at G0/G1 phases and significantly increased caspase-3/-8 without changing caspase-9 levels. The extract showed no toxicity on normal MRC5 lung cells. Non-small-cell lung cancer (NSCLC) A549-induced BALB/c mice were fed with 150 and 300 mg/kg *M. citrifolia* leaf extract and compared with Erlotinib (50 mg/kg body weight) for 21 days. It significantly increased the pro-apoptotic TRP53 genes, down-regulated the pro-tumourigenesis genes (BIRC5, JAK2/STAT3/STAT5A) in the mice tumours, significantly increased the anti-inflammatory IL4, IL10 and NR3C1

expression in the metastasized lung and hepatic cancer tissues and enhanced the NFE2L2-dependent antioxidant responses against oxidative injuries. The extract elevated serum neutrophils and reduced the red blood cells, haemoglobin, corpuscular volume and cell haemoglobin concentration in the lung cancer-induced mammal. It suppressed inflammation and oedema, and upregulated the endogenous antioxidant responses and apoptotic genes to suppress the cancer. The 300 mg/kg extract was more effective than the 50 mg/kg Erlotinib for most of the parameters measured.

Keywords NFE2L2 · Differential counts · IL4 · IL10 · NR3C1 · TRP53 · BCL2

Introduction

Lung cancer is the leading cause of cancer-related death worldwide (1.4 million annually) with a 5-year survival rate of about 14 %. The non-small-cell lung cancer (NSCLC) represents ~80 % of lung cancer cases [1]. Chemotherapy and/or irradiation usually fail because NSCLC cells are intrinsically resistant to them. Chemotherapy is quite ineffective for advanced NSCLC patients with only 20–35 % response rate and a 10- to 12-month median survival [2]. The epidermal growth factor receptor (EGFR) tyrosine kinase inhibitor (TKI) drugs such as Erlotinib improved the overall survival relative to supportive care for refractory stage IIIB/IV NSCLC in a phase III study. However, Erlotinib produces drug resistance and several serious side effects [3] such as shortness of breath, cough, weakness, diarrhoea, rash, appetite loss, fatigue and nausea. Erlotinib may also cause more severe side effects including lung problems (shortness of breath,

Public Interest Statement: This article provides a dietary herbal complementary therapy for lung cancer and compares it with Erlotinib (an FDA-approved lung cancer drug) for their endogenous antioxidant defence, anti-inflammatory and apoptotic effects on the lung cancer cells and development.

✉ Suhaila Mohamed
mohamed.suhaila@gmail.com

¹ UPM-MAKNA Cancer Research Laboratory, Institute of Bioscience, Universiti Putra Malaysia, Level 4, 43400 Serdang, Selangor, Malaysia

² Faculty of Veterinary Medicine, Universiti Putra Malaysia, 43400 Serdang, Selangor, Malaysia

cough and fever); interstitial lung disease; liver and kidney problems; blistering and skin peeling; gastrointestinal perforation; bleeding and clotting problems which may lead to heart attack, stroke, dry eyes, unusual eyelash growth or swelling of the cornea; or harm to an unborn baby and death.

Oxidative stress is usually involved in lung adenocarcinoma development and is responsible for the inflammation in advanced lung cancer patients [4]. SOD2 is an important antioxidant enzyme that protects against oxidative damage in various tissues, by reducing O_2^- , H_2O_2 and OH^- [5]. Inflammation, oxidative stress and oxidative DNA lesions in transformed pulmonary epithelial cells are closely associated with lung cancer development. Oral anti-inflammatory medications often cause side effects such as gastric irritation, ulcer and liver damage [6]. Neutrophils are recruited actively towards the site of injury, but as inflammation resolves, neutrophils may move away from the inflamed site into the circulating bloodstream [7]. Increased neutrophil count is a strong and independent prognostic factor for overall survival, recurrence and cancer-specific survival in patients [8]. Apoptosis (characterized by catabolism and enzymatic cytolysis that facilitate cell morphological changes, such as phosphatidylserine externalization to the cell surface, mitochondrial alterations, membrane blebbing, cell shrinkage, nuclear condensation/fragmentation and separation of apoptotic bodies) is more desirable for anti-cancer therapy than necrosis because inflammation is controlled [9].

The nuclear factor erythroid 2-related factor 2 (NFE2L2 or NRF2) helps alleviate oxidative stress, by inducing nuclear localization and activation of antioxidant response genes. The NFE2L2 is expressed in various human tissues, including lung and liver [10], and is regulated by the Keap1-mediated ubiquitination. The NFE2L2 is protective in several lung inflammatory diseases such as allergen-induced asthma, hyperoxia-induced acute injury, and ventilation-induced acute lung injury [11]. The protective role of NFE2L2-mediated pathway against inflammation is clearly shown in NFE2L2 knockout mice compared with the wild-type mice [12]. NFE2L2 is liver protective against acetaminophen-induced centrilobular hepatocellular necrosis and hepatotoxicity [13]. NFE2L2 would also suppress nitric oxide (NO), cyclooxygenase (COX2) and inducible isoform of nitric oxide synthases (iNOS) [14].

The *M. citrifolia* L. leaves [Noni (Hawaii) or mengkudu (Malay)] are commonly consumed as vegetable by the Polynesians after blanching and are investigated for use as a potential complementary dietary therapy for cancer. It has been reported to enhance immune responses, to be antioxidative and liver protective and to accelerate wound

healing without any acute, sub-acute and sub-chronic oral toxicity [15]. An oral intake of 1000 mg/kg of *M. citrifolia* leaf ethanol extract has been reported as the no-observed-adverse-effect level (NOAEL) [16].

Materials and methods

Plant material

M. citrifolia leaves (Voucher No. SK2322/14, identified by Biodiversity Unit, Institute of Bioscience, Universiti Putra Malaysia, Serdang) were collected from Institute of Bioscience, Universiti Putra Malaysia, State of Selangor, Malaysia. The leaves were dried and mixed in the ratio (w/v) of 1:5 with the 50 % ethanol in water. The yield was 13.61 %. The extracts were analysed by HPLC (Waters 2996, Milford, MA) [17].

Cell Culture and Cell viability assay

Human lung fibroblast (MRC5), human lung adenocarcinoma (A549) cell lines, mouse Lewis (LL2) lung carcinoma cells, Essential Modified Eagle's Medium (EMEM) and Kaighn's Modification of Ham's F-12 (F-12 K) medium were obtained from American Type Culture Collection (ATCC). MRC5, mouse Lewis (LL2) lung carcinoma cells and A549 NSCLC cells were cultured in EMEM and F-12K medium, respectively. All media were supplemented with 10 % foetal bovine serum (PAA, Austria) and 1 % of 100 µg/mL penicillin and streptomycin (Biowest, USA). Cells were grown in a humidified incubator at 37 °C with 5 % CO_2 .

Cells were seeded in 96-well microplates at a density of 2×10^5 cells/mL and treated with Erlotinib (positive control; Cayman, USA) and the extract for 72 h. Then, 20 µL of 5 mg/mL MTT (Nacalai, Kyoto) was added and incubated for 4 h. The absorbance was measured at a wavelength of 595 nm using a microtiter plate reader (Tecan Sunrise basic, Austria) [18].

Acridine Orange (AO)/Propidium Iodide (PI) Double Staining

A549 cells (2×10^5 cells/mL) were treated with IC_{50} concentration of Erlotinib and the extract for 24, 48 and 72 h. 10 µL of AO/PI dyes (Biotium, USA), containing AO (10 µg/mL) and PI (10 µg/mL), were added into the cellular pellet, and then observed under fluorescence microscope with 200x magnification (Leica attached with Q-Floro Software; Wetzlar, Germany) [18].

Cell cycle analysis

A549 cells (2×10^5 cells/mL) were treated with IC_{50} concentration of Erlotinib and the extract. After 12, 24, 48 and 72 h of incubation, the cells were trypsinized, washed, fixed in 70 % ethanol, stained with 1 mg/mL PI and analysed by flow cytometry (BD FACS Canto II, USA) [18].

Caspase-3, -8 and -9 Bioluminescent Assays

A549 cells (2×10^6 cells/mL) were plated in 75 cm³ culture flasks and treated with Erlotinib and the extract at their IC_{50} values, respectively, for 24, 48 and 72 h. The cells were lysed and then 50 µL of 2× reaction buffer and 5 µL of DEVD-pNA were added (caspase-3, -8 or -9 substrate; Genscript, USA). After incubation at 37 °C for 1 h, the samples were read at 405 nm by a microplate reader (TECAN, Männedorf, Switzerland).

Animal study and ethics statement

The animal studies were conducted strictly according to the Guidelines of the Institutional Animal Care and Use Committee (IACUC), Universiti Putra Malaysia (protocol approval number: UPM/IACUC/AUP-R016/2013).

In vivo tumour xenograft model

Six-week-old male BALB/C mice (weighing 19–20 g) were purchased from Faculty of Veterinary Medicine, Universiti Putra Malaysia, and housed in cages under a 12-h light/dark cycle. Ten healthy mice were selected and assigned as Group I. Next, A549 NSCLC cells (2×10^7) suspended in 100 µL PBS were injected subcutaneously into the backs of forty mice [19]. When the tumour size reached approximately 100 mm³, after 14 days of implantation, the mice were randomly assigned to the following experimental groups and administered daily by oral gavage for 21 days: saline (Group II), Erlotinib (50 mg/kg) (Group III), 150 mg/kg (Group IV) and 300 mg/kg (Group V) of *M. citrifolia* leaves.

Mice were sacrificed via intraperitoneal injection of ketamine HCl (100 mg/kg) and xylazine (10 mg/kg). Lung and liver tissues were excised and some were snap frozen in liquid nitrogen for gene expression, while the others were fixed in 10 % formalin and embedded in paraffin for haematoxylin and eosin (H&E) staining. The inflammation scores were evaluated under the microscope (Leica DM-LB2, Solms, Germany). The “Z” shape was drawn at the middle of the images, and then divided into 20 fields to count the percentage of inflammation areas. Blood samples were collected in EDTA-coated collection tubes for differential counts. Blood cells were stained using ABBOT

reagent and analysed in ABBOT Celldyn 3700 (Geliga Sistem Sdn Bhd, Petaling Jaya, Malaysia).

Gene expression

The tumour, lung and liver RNA were isolated using Trizol (Invitrogen, Carlsbad, CA). Custom RT² Profiler PCR Array (CAPM11988), RT² SYBR Green qPCR Mastermix, RT² First Strand Kit and RNase-Free DNase Set were purchased from SuperArray Bioscience Corporation (Frederick, MD). Quantitative RT-PCR array for differentially expressed genes was performed utilizing RT² Profiler PCR Array Data Analysis version 3.5 (SABiosciences; Frederick, MD, USA), which normalized to HSP90AB1 (NM_008302) and GAPDH (NM_008084). RT-PCR data are represented as the average relative mRNA gene expression of each experimental group ($n = 3$). Fold change ($2^{(-\Delta\Delta C_t)}$) is defined as the normalized gene expression ($2^{(-\Delta C_t)}$) in the test sample, divided by the normalized gene expression ($2^{(-\Delta C_t)}$) in the control sample. Fold regulation represents fold change as biologically meaningful results. Fold change values greater than one indicate a positive- or an upregulation, and the fold regulation is equal to the fold change. Fold change values less than one indicate a negative or down-regulation, and the fold regulation is the negative inverse of the fold change. The p values are calculated based on a t test of the replicate $2^{(-\Delta C_t)}$ values for each gene in the control mice and treatment groups.

Statistical analysis

Data were expressed as mean \pm standard deviation (mean \pm SD) of at least three independent experiments; significant differences ($p < 0.05$) were tested using one-way analysis of variance (ANOVA) and Duncan test using statistical analysis IBM SPSS Statistics 21 software.

Results

M. citrifolia leaf extract showed antiproliferative effect on A549 lung cancer cells without affecting normal MRC5 lung cells

The extract and Erlotinib were selectively cytotoxic to lung cancer cells but not to non-cancerous MRC5 lung cells even at 100 µg/mL (Fig. 2a). *M. citrifolia* leaf 50 % ethanolic crude extract was strongly cytotoxic towards A549 and LL2 cells with IC_{50} values of 23.47 and 5.50 µg/mL, respectively (Fig. 1b), which were only 2–8 times higher than Erlotinib (IC_{50} of 2.83 µg/mL). The time-dependent apoptotic effect of the extract was subsequently based on this IC_{50} value for A549.

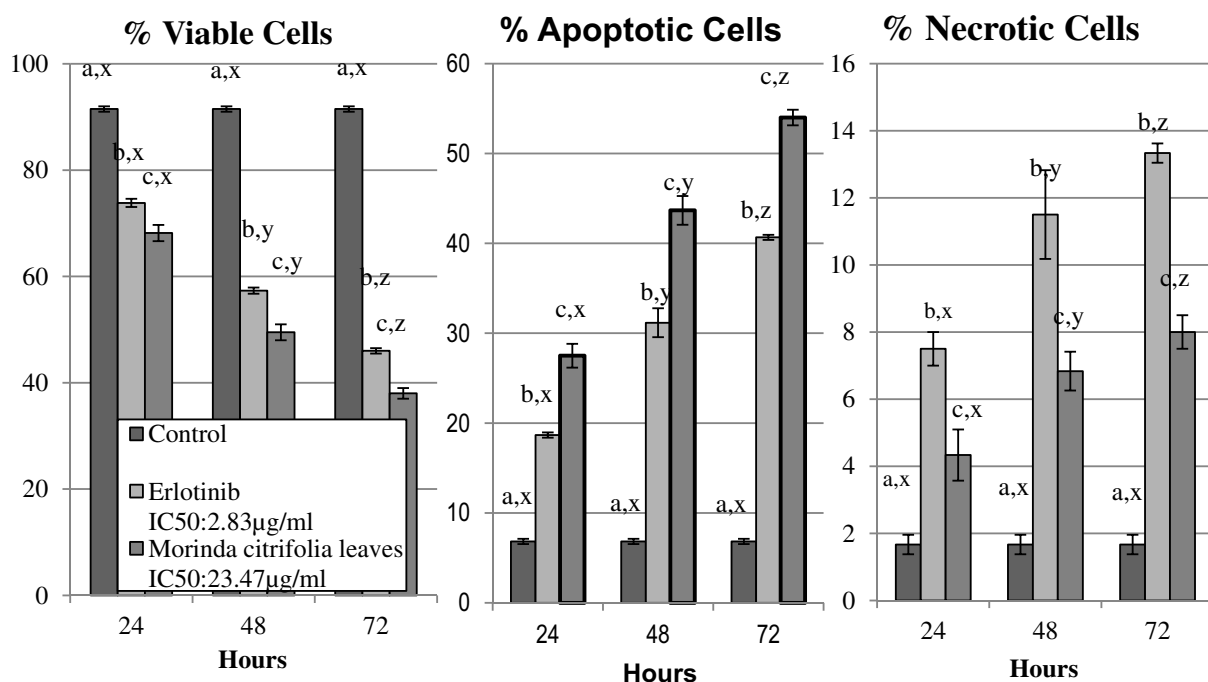
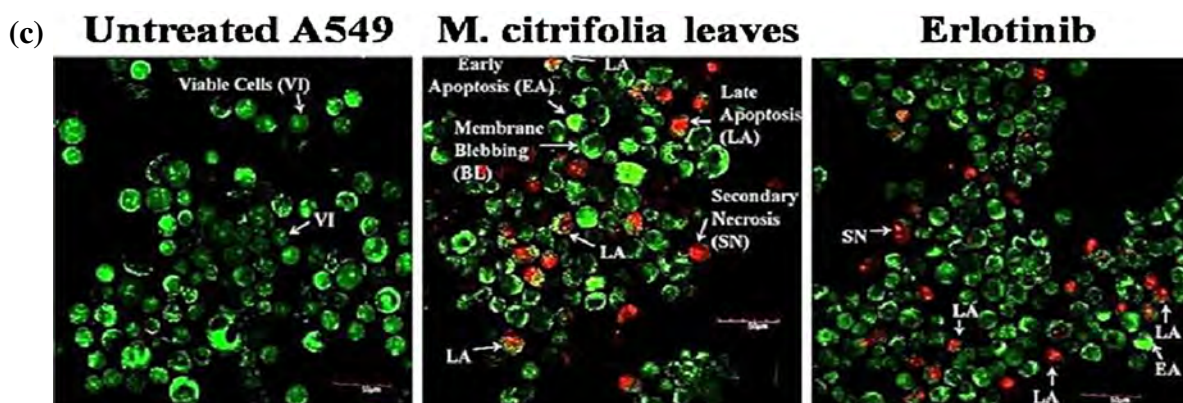
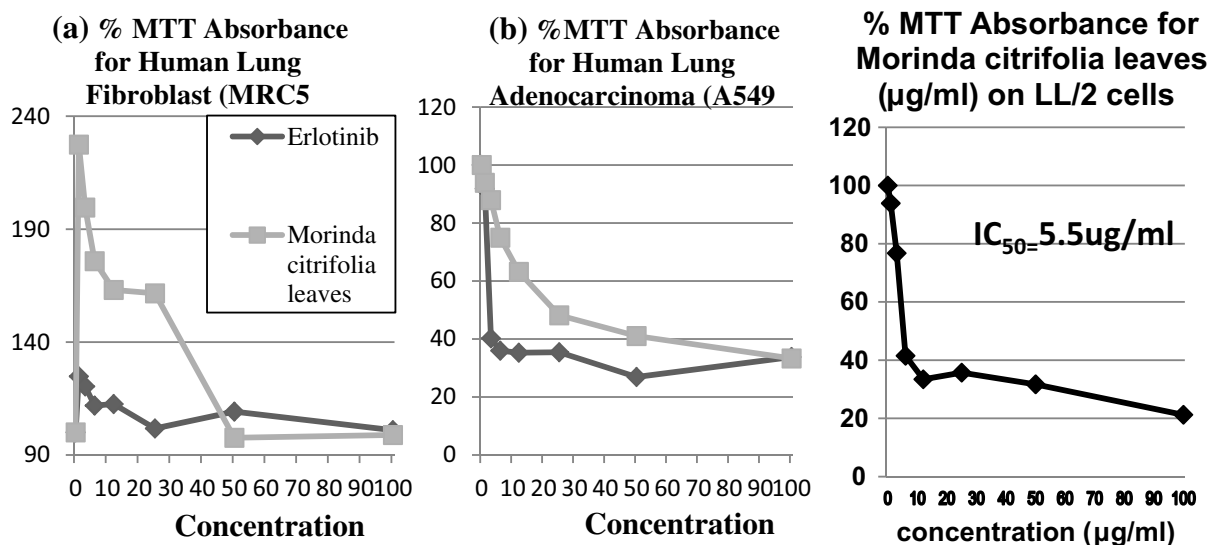


Fig. 1 Viability of **a** normal MRC5 cells and **b** lung cancer A549 cells (% MTT Absorbance) and LL-2 after 72-h treatment with the IC₅₀ values of leaf extract or Erlotinib; and fluorescence micrograph (**c, d**) of treated A549 cells. [**c** Cells exhibit blebbing of the cell membrane and bright green nucleus showing condensation of chromatin; early apoptotic features were seen by representing intercalated AO (*bright green*) amongst the fragmented DNA; *orange colour* represents the hallmark of late apoptosis, while *red colour* represents secondary necrosis or dead cells after 72-h treatment. *VI* viable cells; *BL* blebbing of the cell membrane; *EA* early apoptosis; *LA* late apoptosis; *SN* secondary necrosis (200× magnification). **d** Both treatments enhanced apoptosis event in A549 cells significantly ($p < 0.05$) in a time-dependent manner. Data are shown as mean \pm SD ($n = 3$). **a, b, c* differed significantly at $p < 0.05$ across treatment groups with time as compared with control; *x, y, z* differed significantly at $p < 0.05$ across time within treatment group as compared with control]

***M. citrifolia* leaf extract induced apoptotic morphological changes**

The AO/PI double staining to semi-quantitate the viable, apoptotic and necrotic cells showed morphological changes in the cells upon treatment (Fig. 1c, d). Untreated A549 cells showed even distribution of the acridine orange stain as green intact nucleus (denotes healthy cells) with well-preserved morphology. After treatment of the extract, blebbing of the cell membrane and dense green nucleus, which indicated nuclear chromatin condensation, were noticeable. Both early apoptotic features (blebbing and chromatin condensation) and late apoptotic phases (intense reddish-orange colour due to acridine orange binding to denatured DNA) were apparent after 72 h.

***M. citrifolia* leaf extract induced G0/G1 arrest and activated extrinsic caspase activity**

Both the extract and Erlotinib induced G0/G1 phase cell cycle arrest in A549 cells (Fig. 2a), which was accompanied by a concomitant decrease in both S and G2/M phase cells. The extract and Erlotinib significantly ($p < 0.05$) increased the caspase-3 and -8 activities (Fig. 2b) in a time-dependent manner, whilst the activity of caspase 9 remained unchanged throughout the treatment period in comparison with the untreated cells. This suggested that *M. citrifolia* leaf extract induced apoptosis in A549 cells via the death receptor pathway.

***M. citrifolia* leaf extract suppressed tumour growth in vivo**

The effect of the extract on lung cancer growth is shown in Fig. 3. The 300 mg/kg extract potently suppressed the tumour volume better than the 50 mg/kg Erlotinib, while the 150 mg/kg extract only inhibits about 50 % of the

tumour growth (Fig. 3a). The H&E staining on the A549 xenograft mice tissues showed nodular cancer cell mass (Fig. 3b), whereas the immunohistochemical (IHC) labelling of tumour sections shows positive EGFR staining (Fig. 3c), indicating a good correlation between the tumour EGFR molecules and their IHC EGFR status, as previously reported [20].

Histopathology observations for lung and liver inflammation

All the mice survived until the end of experiment (zero mortality). The untreated cancer-induced mice showed the highest inflammation scores in both lung (67 ± 1 %) and liver (53 ± 2 %) as compared to the healthy control mice and other groups (Fig. 4). Extensive inflammation by monocytes, oedema in the lung parenchyma and extensive hepatocellular necrosis in liver were seen in the untreated cancer-induced mice. For both the lungs and the liver, the 150 mg/kg extract reduced these severe inflammation conditions. The 300 mg/kg extract and 50 mg/kg Erlotinib were very effective in reducing inflammation in both the lungs and the livers; the 300 mg/kg extract was two times more effective than the 50 mg/kg Erlotinib treatment.

Blood differential counts

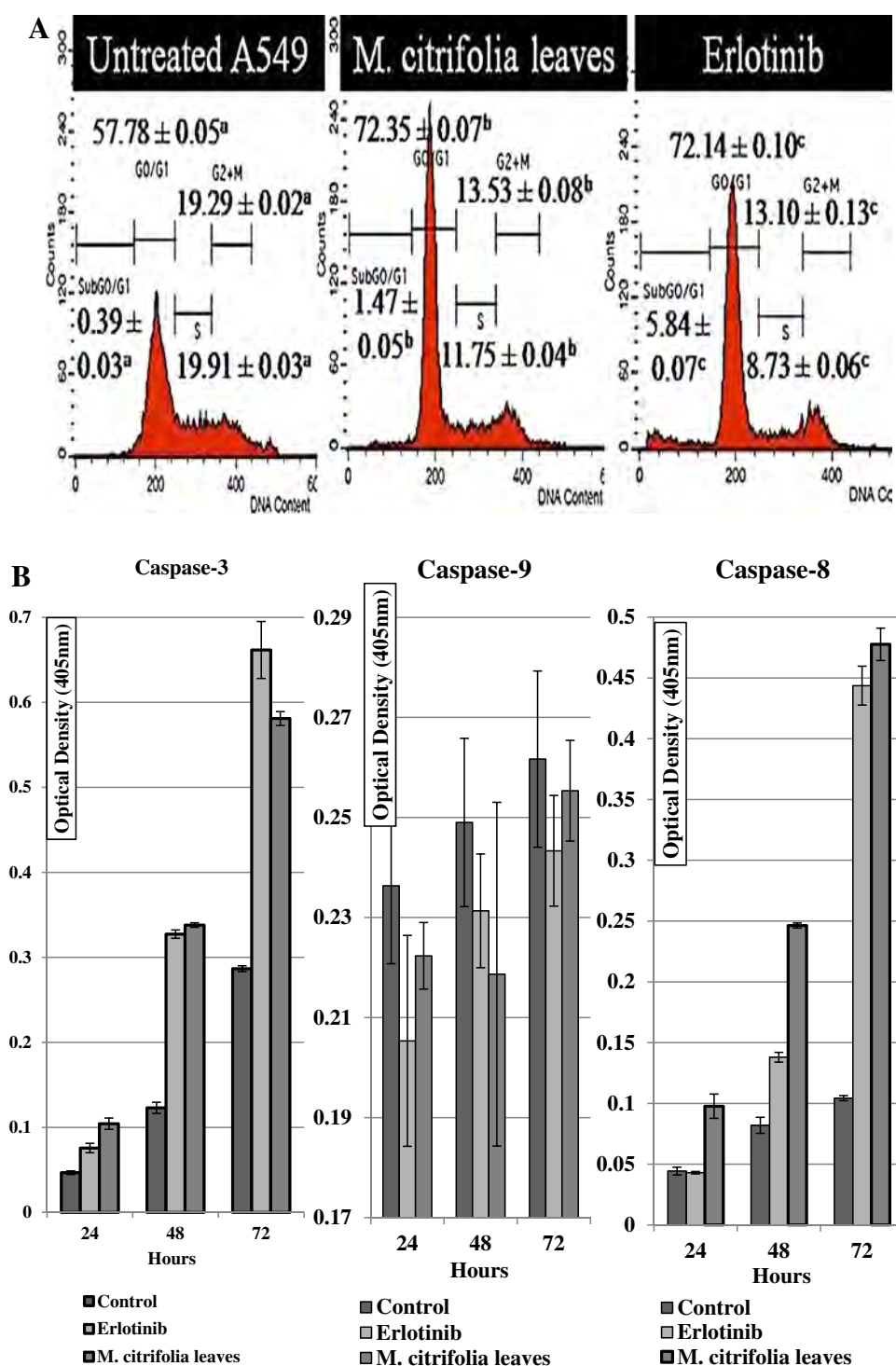
The untreated cancer-induced mice had lower red blood cells (RBCs), haemoglobin (Hb), mean corpuscular volume (MCV), mean cell haemoglobin concentration (MCHC) and segmented/banded neutrophil values as compared to the other groups (Fig. 5). The 300 mg/kg extract recorded $9.9 \pm 0.2 \times 10^{12}/L$ in RBC, 150.5 ± 1.5 g/L in Hb, 44.3 ± 0.6 fL in MCV and 377.7 ± 5.2 g/L in MCHC, which was significantly higher than Erlotinib and 150 mg/kg extract.

The untreated cancer-induced mice had the lowest banded/segmented neutrophil counts, while the control healthy mice had a higher neutrophil counts. Administration of 150 mg/kg extract significantly enhanced the segmented neutrophils, but not banded neutrophil levels relative to the untreated cancer-induced mice. The 300 mg/kg extract significantly increased segmented/banded neutrophil counts as compared with the untreated cancer-induced mice.

***M. citrifolia* leaf extract upregulated pro-apoptotic, anti-inflammatory and antioxidant-related genes expression**

The extract improved the body weight and suppressed the tumour volume better than Erlotinib (Fig. 6). The *M. citrifolia* leaf extract treatment to the cancer-induced mice

Fig. 2 Cell cycle and caspase-3/-8/-9 on treated A549 cells. **a** Flow cytometric analysis of cell cycle phase distribution of treated A549 cells after 72 h based on their IC₅₀ values, respectively. Sub-G0/G1 peak denoting apoptotic cells with hypodiploid DNA content, and followed by G0/G1, S, and G2/M phases. Both extract and Erlotinib induced G0/G1 arrest in cell cycle progression in A549 cells. **b** Relative luminescence expression of caspase-3, -8 and -9 in treated A549 cells, with their IC₅₀ values, respectively. Caspase-3 and -8 were significantly increased in both extract and Erlotinib as compared to the untreated cells. (All data are shown as mean \pm SD ($n=3$). **a*, *b*, *c* differed significantly across treatment groups at $p < 0.05$ with time as compared with control; *x*, *y*, *z* differed significantly across time at $p < 0.05$ within treatment group as compared with control)]



dose-dependently decreased JAK2/STAT3/STAT5A and BIRC5 expressions, and significantly ($p < 0.05$) enhanced TRP53 (Fig. 6) on the tumour tissues, similar to Erlotinib. Although the TRP53 was significantly upregulated in Erlotinib-treated mice (1.19-fold), its gene expression was lower as compared with 300 mg/kg of *M. citrifolia* leaf extract (4.19-fold) treatment.

The 300 mg/kg extract treatment to the cancer-induced mice significantly increased both anti-inflammatory (IL4, IL10, NR3CL) and antioxidant markers (SOD2, NFE2L2), both in the lung and hepatic tissues (Fig. 6). Erlotinib significantly upregulated the IL4 in both the lung and liver, with 3.33-fold ($p = 0.01$) and 2.07-fold ($p = 0.04$), respectively. The 150 mg/kg extract significantly enhanced

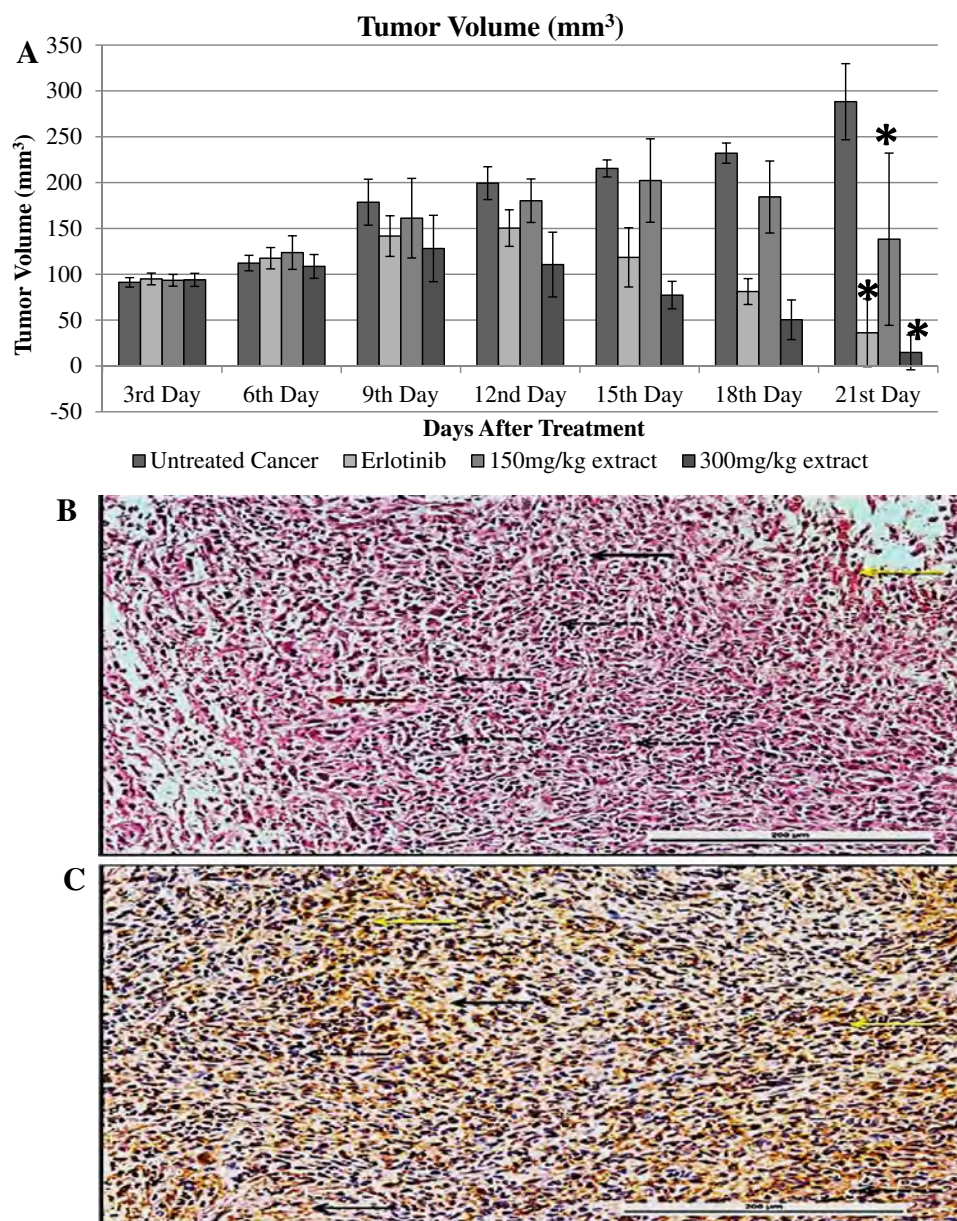


Fig. 3 Tumour volumes (a) of cancer-induced mice with and without treatment with 150–300 mg/kg extract or 50 mg/kg Erlotinib, and H&E (b)/IHC (c) staining for EGFR expression. [b] H&E staining of tumour tissue (Magnification, $\times 200$). Pleomorphic-hyperchromatic cells with different size and shape can be seen in the given section (black arrow). The cells are oriented in multiple directions with cord-like and cluster-like patterns of growth given the section the so-called poorly differentiated tumour (dashed black arrow). Newly formed blood vessels (angiogenesis) can be seen in the upper right part merging toward the tumour mass (yellow arrow). Massive pinkish amorphous extracellular matrix distributed diffusely within the

tumour mass mixed with proliferated collagen connective tissue supporting stroma (red arrow). [c] IHC staining for EGFR expression on tumour tissues (Magnification, $\times 200$). Photomicrograph representing immunohistochemical (IHC) staining with EGFR revealed extensive immunopositive reaction in the stromal supportive tissue of tumour mass indicated by the presence of deep to light golden brown colour within the section (black arrow). Some of the tumour cells showed immunopositive reaction indicated in deep-brown colour (yellow arrow). Higher percentage of tumour cells showed immunonegative reaction to EGFR indicated by their counter stained haematoxylin blue colour (dashed black arrow)]

the NFE2L2 (2.23-fold, $p = 0.04$) in lung and SOD2 (2.88-fold, $p = 0.01$) in liver tissues. The 300 mg/kg extract was more effective in activating pro-apoptotic, anti-inflammatory and antioxidant-relevant gene expression in selected tissues, as compared to the 50 mg/kg Erlotinib.

Discussion

The *M. citrifolia* 50 % ethanolic extract contained 2.19 % scopoletin (retention time, $R_t = 12.02$ min) and 3.41 % epicatechin ($R_t = 9.17$ min). Spiking with scopoletin and

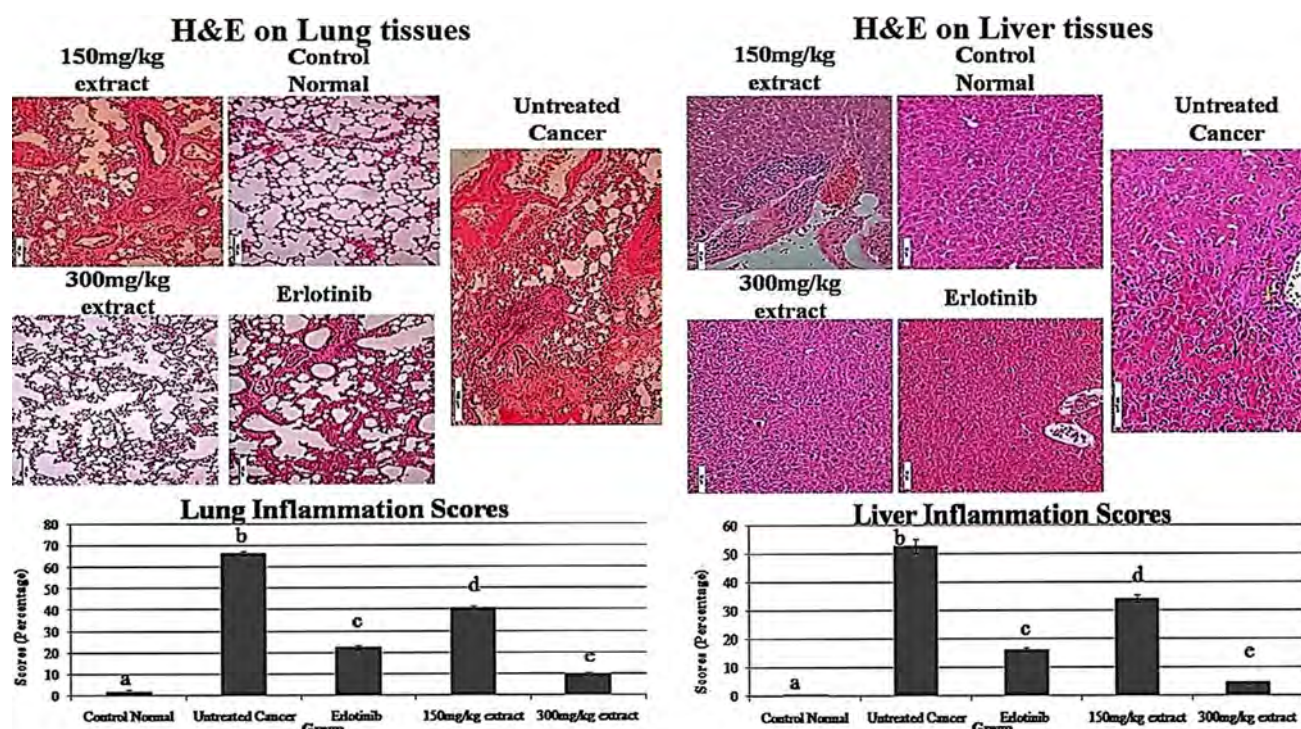


Fig. 4 Inflammation of the lungs and livers with different treatments. [Lung parenchyma from untreated cancer group shows extensive inflammation by monocytes and oedema characterized by alveolar wall thickening, infiltration of inflammatory cells, interstitial and airspace oedema and capillary congestion. However, these changes were less severe in the 150 mg/kg extract and Erlotinib groups, while that of the 300 mg/kg extract group resembled that of the control

(H&E, $\times 100$). Extensive inflammations along with extensive hepatocellular necrosis were seen in the livers of the untreated cancer-induced group. The changes were comparatively less severe in the 150 mg/kg extract, while those of the Erlotinib and 300 mg/kg extract group have similar histology as that of the healthy controls (H&E, $\times 200$). Values are expressed as mean \pm SD ($n = 3$). Means with different superscripts are significantly different ($p < 0.05$)]

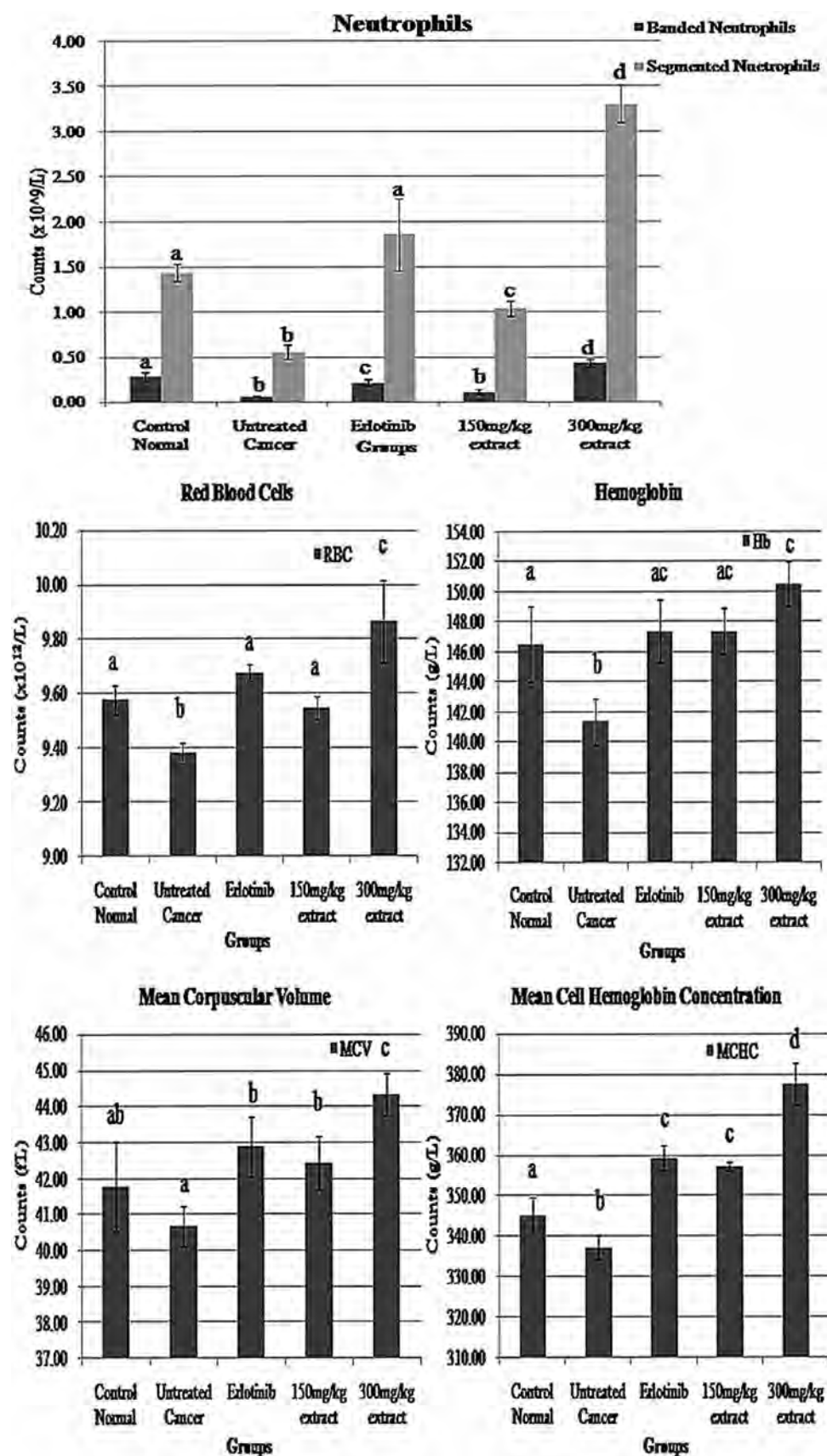
epicatechin produced sharp extended peaks at the specific retention times which qualitatively confirmed them [21]. Scopoletin reportedly inhibited cancer cell proliferation by (i) inducing cell cycle arrest in G0/G1 and S phases, and increased apoptosis in human prostate tumour PC3 cells [22], (ii) induced NF κ B activation and apoptosis in human promyeloleukemic (HL-60) cells by activating caspase-3, and PARP degradation [23]. Epicatechin showed in vitro anti-human lung cancer (PC-9) cells [24]. Epicatechin and catechin were less cytotoxic than other catechins [epicatechin gallate (ECG), catechin-gallate (CG), epigallocatechin gallate (EGCG) and epigallocatechin (EGC)] in HSC-2 carcinoma cells and HGF-2 fibroblasts [25]. Therefore, the anti-cancer effects of *M. citrifolia* leaf extract may be a synergetic action by these compounds.

The *M. citrifolia* leaf extract 50 % inhibition (IC_{50}) in A549 cells was 23.47 μ g/mL, which was better than those of green tea extract ($IC_{50} = 112.00$ μ g/mL) or ginger extract ($IC_{50} = 239.4 \pm 7.4$ μ g/mL) [26], and below the crude extracts' potency ($IC_{50} < 30$ μ g/mL after 72-h exposure) set by the American National Cancer Institute guidelines [27]. Polyphenolic compounds in food usually

inhibited the growth and induced apoptosis of cancer cells at relatively high concentrations of >30 μ M.

Most lung adenocarcinomas express EGFR protein for tumour growth, infiltration and metastasis, which is routinely monitored in clinical practice for mutations and improved response to EGFR TKI [28]. Here, the IHC staining showed positive EGFR expression on A549-tumour-induced mice model, indicating successful tumour growth and invasion by the xenograft technique used, consistent with previous patient analyses where the EGFR protein is expressed in 60–90 % of NSCLC tumours [29]. Erlotinib was used as a comparison drug because it is a potent, reversible and selective inhibitor of the EGFR tyrosine kinase, which blocks cell cycle progression in the G1 phase. It also prevents inflammatory response, TGF α , and iNOS mRNA expressions, inhibits human umbilical vein endothelial cell (HUVEC) growth and xenograft vessel density and is approved as a late-stage development therapeutic agent that targets angiogenesis in the treatment of NSCLC. Erlotinib is the only FDA-approved EGFR TKI in the United States for patients with locally advanced or metastatic NSCLC [30].

Fig. 5 Blood differential counts on different experimental groups. [Values are expressed as mean \pm standard deviation ($n = 3$). Means with different superscripts are significantly different ($p < 0.05$)]



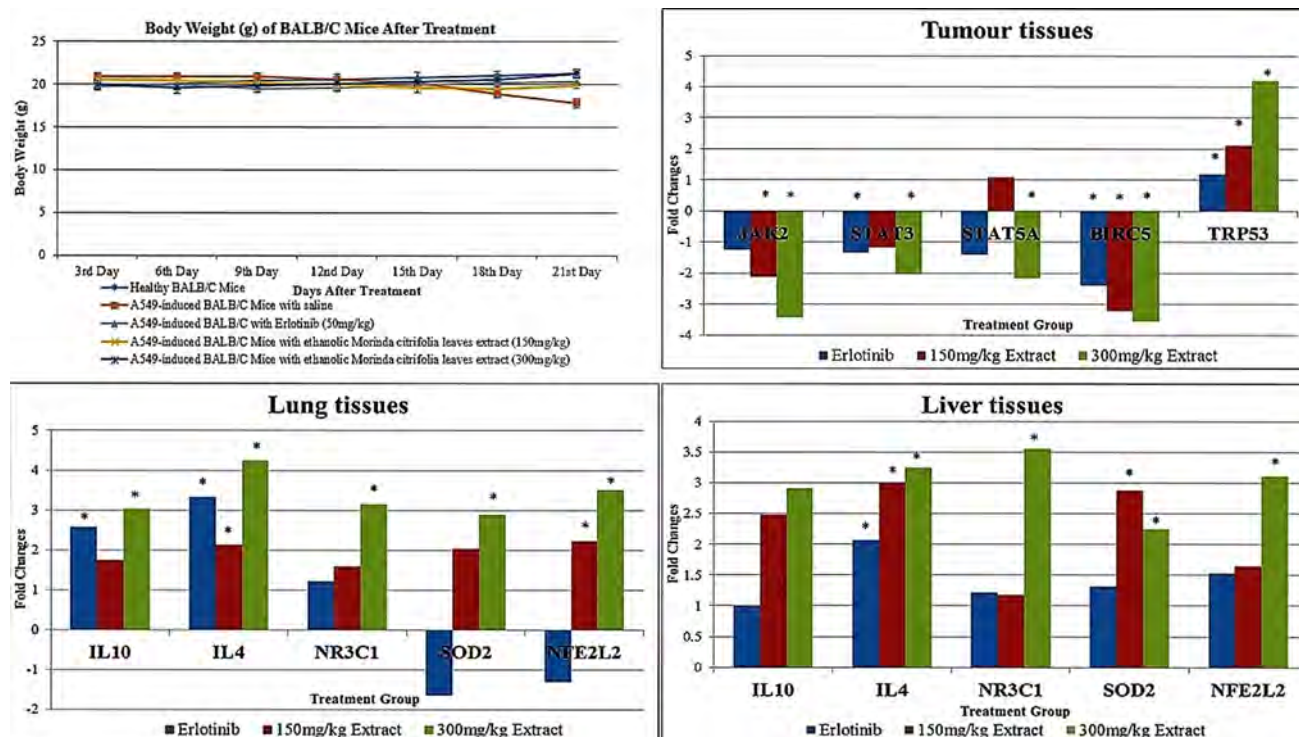


Fig. 6 Body weights and quantitative RT-PCR array for gene expression in mouse tumour, lung and liver tissues. {[Gene: Accession Number, Description]. Jak2: NM_008413, Janus kinase 2; Stat3: NM_011486, Signal transducer and activator of transcription 3. Stat5a: NM_011488, Signal transducer and activator of transcription 5A; Birc5: NM_009689, Baculoviral IAP repeat-containing 5; Trp53: NM_011640, Transformation-related protein 53; IL10: NM_010548, Interleukin 10; IL4: NM_021283, Interleukin 4; NR3C1: NM_008173, Nuclear receptor subfamily 3, group C, member 1; SOD2: NM_013671, Superoxide dismutase 2, mitochondrial;

NFE2L2: NM_010902, Nuclear factor, erythroid-derived 2, like 2; IL10: NM_010548, Interleukin 10; IL4: NM_021283, Interleukin 4; NR3C1: NM_008173, Nuclear receptor subfamily 3, group C, member 1; SOD2: NM_013671, Superoxide dismutase 2, mitochondrial; NFE2L2: NM_010902, Nuclear factor, erythroid-derived 2, like 2. Quantitative RT-PCR analysis was performed using the comparative threshold cycle method to calculate fold change in gene expression normalized to GAPDH and HSP90AB1 as a reference gene. Values represent fold change between control and treatment groups}

The extract strongly upregulated the TRP53 genes in the mice tumours, which favours p53 nuclear translocation and transcriptional targets activation such as P21 and BAX regulated cell cycle control and apoptosis [31]. The p53-mediated apoptosis was also associated with the caspase-3 and -8 extrinsic apoptotic pathways' activation and BCL2 expression reduction [32]. The extract showed extrinsic apoptotic cytotoxic effects only on the A569 cancer cells, via the caspase-3 and -8 cascade pathways. DNA damage and other stress signals may trigger the increase of p53. In the current study, P53 upregulated expression was linked to the reduced MDM2 levels. The MDM2 negatively controls P53 stability, function and concentration by (I) preventing P53 transcription through binding via protein–protein interactions to the P53N-terminal transcription activation domain, (II) promoting P53 degradation by ubiquitin-dependent proteasomal degradation and acting as an E3 ubiquitin ligase and (III) causing nuclear export of P53 into

the cell cytoplasm, away from its action site [33]. The P53-dependent apoptosis is induced by the caspase proteases and death receptors, and functions through pro-apoptotic proteins including BAX (BCL2-associated X protein), NOXA (phorbol-12-myristate-13-acetate-induced protein 1) or PUMA (P53-upregulated modulator of apoptosis).

The 300 mg/kg *M. citrifolia* leaf extract downregulated survivin expression, the gene that supports chemo- and radio-resistance [34]. The survivin suppression consequently subdued NFkB, PI3 K/AKT and MTOR pathways, and discouraged cancer cell proliferation and survival. High survivin expression is frequent in lung adenocarcinomas and was associated with decreased NSCLC patient survival [35]. The *M. citrifolia* leaves may also help sensitize lung adenocarcinoma to chemo- and radiation therapy as a complementary treatment.

The extract effectively targeted the JAK2, with subsequent prolonged loss of STAT3/STAT5A signalling to

inhibit the invasion of lung adenocarcinoma. The sustained inhibition of the JAK/STAT signalling axis by *M. citrifolia* leaves was more effective than Erlotinib at the doses used. NSCLC surgery patients with high JAK2 expression have poor overall survival rate compared to those with low JAK2 expression [36]. The main substrates for JAK2 frequently implicated in human cancer progression are STAT3 and STAT5A that are activated in about 55 and 33 % of NSCLC tumours, respectively [37]. STAT3 promotes (i) tumour cell growth, angiogenesis and apoptosis resistance to chemotherapeutic agents, (ii) cyclin D1 and cMyc upregulation, to accelerate cell cycle progression, (iii) survival signals and BCL2, BCLXL, MCL1, survivin and cIAP expressions and (iv) down-regulates P53 expression [38], while STAT5A activates BCL2/BCLXL [39]. Hence, *M. citrifolia* leaf-induced TRP53 upregulated expression was also linked to the reduced STAT3 levels.

The extract suppressed the extensive inflammation in both the lung and liver tissues, which is evident from the histopathology results. The 300 mg/kg *M. citrifolia* leaf 50 % ethanolic extract was apparently more effective than the 50 mg/kg Erlotinib in suppressing these parameters. Inflammation and inflammatory cell infiltration appeared abundantly in the direct vicinity of resected tumours. The increased circulating blood neutrophil counts with the 300 mg/kg dose leaf extract consumption in the cancer-induced mice appeared better than that with the 50 mg/kg Erlotinib. The untreated cancer-induced mice had low circulating RBC which again reflects inflammation. The leaf extract dose-dependently increased the circulating RBC differential counts in the cancer-induced mice to near normal levels, indicating its anti-inflammatory effects. The low circulating RBC levels are triggered by inflammation and changes in erythropoiesis [40]. Red blood cell values were negatively associated with clinical cancer stage and poorer prognoses [41].

Consistently, the leaf extract treatment dose-dependently enhanced IL4, IL10 and NR3C1 expression in both the lung and liver tissues to support the anti-inflammatory and anti-angiogenesis effects against cancer growth. The IL4 suppressed (1) macrophage cytotoxic activity and macrophage-derived nitric oxide production [42], (2) the matrix metalloproteinase 9 expression, which is an initial step in cancer invasion [43], and (3) the tumour-associated fibroblast activation, which are important promoters of tumour growth and progression [44]. The absence of IL10 expression by the tumour was associated with a poor survival in patients with stage I NSCLC [45]. Transfection of IL10 to mouse carcinoma and melanoma cell lines elicited tumourigenicity loss and increased immunogenicity accompanied by a strong lymphocyte- and antibody-dependent immune memory [46]. The IL10 antitumour

effects were linked to enhanced natural killer cell activity, and depended on CD8+ or CD4+ T-cell functions [47]. Other foods such as chili pepper have also been shown to enhance the IL10 secretion to 190 % in a lipopolysaccharide-stimulated macrophage model [48]. Moreover, the glucocorticoid receptor (GR), encoded by NR3C1, exhibits anti-inflammatory effects through transcriptional activation of glucocorticoid-induced leucine zipper genes or transcriptional suppression of genes of inflammatory cytokines induced by nuclear factor- κ B (NF κ B) or activator protein-1 (AP-1) [49]. Scopoletin and epicatechin, in the *M. citrifolia* leaf extract, have strong antioxidant properties [50, 51]. The leaf extract treatments upregulated the SOD2 expressions in both the lung and liver tissues in cancer-induced mice, better than Erlotinib, and may help improve the capacity to detoxify O₂⁻.

M. citrifolia leaf extract also induced NFE2L2 expressions in both the lung and liver tissues, signifying its potent antioxidant-inducing properties. NFE2L2 stimulation would significantly upregulate its target genes, such as glutamate-cysteine ligase catalytic (GCLC) and modulator (GCLM) subunits of the rate-limiting enzyme in glutathione biosynthesis (glutamate-cysteine ligase), detoxification enzymes [glutathione S-transferase (GST) and NAD(P)H:quinone oxidoreductase 1 (NQO1)] and antioxidant enzymes [glutathione peroxidase (GPx) and catalase (CAT), SOD and heme oxygenase-1 (HO-1)] by binding to their antioxidant response element (ARE) present in these gene promoters. Epicatechin reportedly protects neurons against oxidative insults through the NFE2L2–HO1 pathway [52]. The extract caused significant enhancement of the anti-inflammatory, antioxidant and apoptotic biochemical markers, suggesting a mode of action targeting multiple signalling pathways in vivo (shown in Fig. 7).

In conclusion, the *M. citrifolia* leaves inhibited the A549 NSCLC cell proliferation and survival ability by inducing G0/G1 cell cycle arrest and extrinsic apoptotic pathway. Oral administration of *M. citrifolia* leaves decreased the tumourigenicity of malignant A549 lung cancer, by significantly increasing TRP53 gene expression, and concomitantly decreasing the anti-apoptotic BIRC5 and JAK2/STAT3/STAT5A genes. The scopoletin- and epicatechin-rich *M. citrifolia* leaf extract supplementation to lung cancer-bearing mice also demonstrated anti-inflammatory and antioxidant effects by increasing the efflux of inflamed tissues, enhancing inflammatory cell clearance, suppressing oedema accumulation and inhibiting oxidative stress. Taken together, these evidences suggest that the *M. citrifolia* leaf extract may be a complementary therapy or functional food in the prevention or management of lung cancer inflammation, oxidative stress, growth and metastasis.

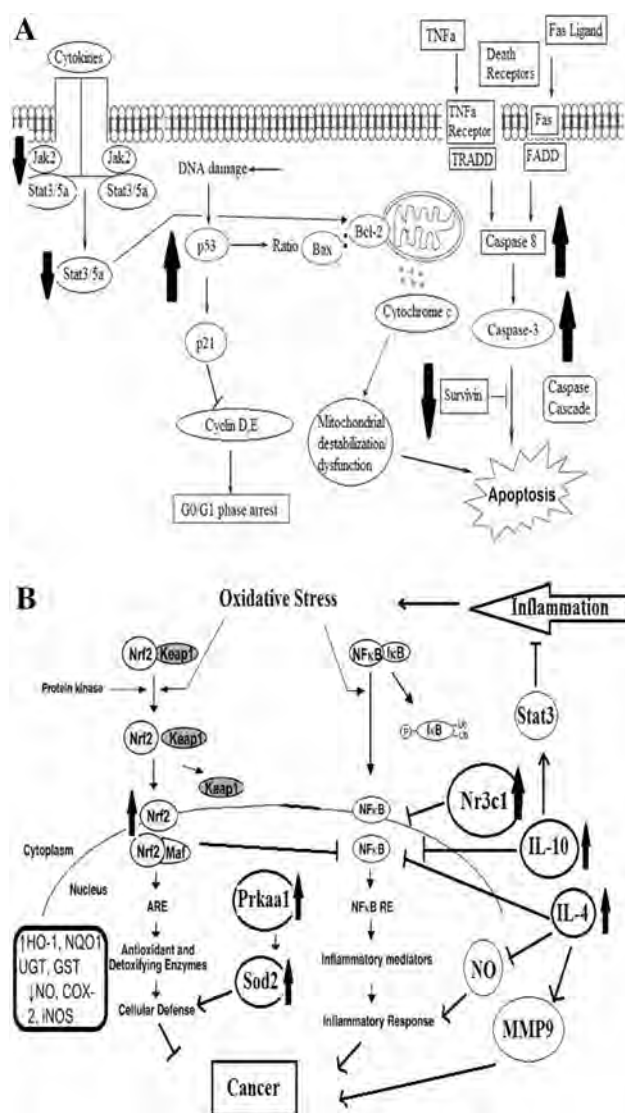


Fig. 7 **a** Proposed model of *M. citrifolia* leaf extract mechanism of action for G0/G1 arrest and apoptosis in vitro and in vivo; **b** a simplified illustration showing the role of *M. citrifolia* leaf extract in antioxidative and anti-inflammatory pathways preventing lung adenocarcinoma in vivo

Acknowledgments This study was supported by the Herbal Development Office, Ministry of Agriculture (Grant No. NH05135009).

Compliance with ethical standards

Conflicts of Interest The authors declare no conflict of interest.

References

- Jemal A, Bray F, Center M (2011) Global cancer statistics. *CA Cancer J Clin* 61:69–90
- Spiro S, Tanner N, Silvestri G et al (2010) Lung cancer: progress in diagnosis, staging and therapy. *Respirology* 15:44–50
- Politi K, Fan P, Shen R et al (2010) Erlotinib resistance in mouse models of epidermal growth factor receptor-induced lung adenocarcinoma. *Dis Model Mech* 3:111–119
- Forrest L, McMillan D, McArdle C et al (2003) Evaluation of cumulative prognostic scores based on the systemic inflammatory response in patients with inoperable non-small-cell lung cancer. *Br J Cancer* 89:1028–1030
- Lim C, Junit S, Abdulla M, Aziz A (2013) In vivo biochemical and gene expression analyses of the antioxidant activities and hypocholesterolaemic properties of tamarindus indica fruit pulp extract. *PLoS ONE* 8:e70058
- Amir M, Javed S, Kumar H (2010) Design and synthesis of 3-[3-(substituted phenyl)-4-piperidin-1-ylmethyl]-4-morpholin-4-yl-methyl-4,5-dihydro-isoxazol-5-yl]-1H-indoles as potent anti-inflammatory agents. *Med Chem Res* 19:299–310
- Holmes G, Dixon G, Anderson S, et al. (2012) Drift-diffusion analysis of neutrophil migration during inflammation resolution in a zebrafish model. *Advances in hematology*, vol. 8
- Trellakis S, Farjah H, Bruderek K et al (2010) Peripheral blood neutrophil granulocytes from patients with head and neck squamous cell carcinoma functionally differ from their counterparts in healthy donors. *Int J Immunopathol Pharmacol* 24:683–693
- Kanduc D, Mittelman A, Serpico R et al (2002) Cell death: apoptosis versus necrosis (Review). *Int J Oncol* 21:165–170
- Hu Y, Ju Y, Lin D et al (2012) Mutation of the Nrf2 gene in non-small cell lung cancer. *Mol Biol Rep* 39:4743–4747
- Papaiahgari S, Zhang Q, Kleeberger S et al (2006) Hyperoxia stimulates an Nrf2-ARE transcriptional response via ROS-EGFR-PI3K-Akt/ERK MAP kinase signaling in pulmonary epithelial cells. *Antioxid Redox Signal* 8:43–52
- Li W, Khor T, Xu C et al (2008) Activation of Nrf2-antioxidant signaling attenuates NFκB-inflammatory response and elicits apoptosis. *Biochem Pharmacol* 76:1485–1489
- Enomoto A, Itoh K, Nagayoshi E et al (2001) High sensitivity of Nrf2 knockout mice to acetaminophen hepatotoxicity associated with decreased expression of ARE-regulated drug metabolizing enzymes and antioxidant genes. *Toxicol Sci* 59:169–177
- Kim H, Vaziri N (2010) Contribution of impaired Nrf2-Keap1 pathway to oxidative stress and inflammation in chronic renal failure. *Am J Physiol* 298:F662–F671
- West B, Tani H, Palu A et al (2007) Safety tests and antinutrient analyses of noni (*Morinda citrifolia* L.) leaf. *J Sci Food Agric* 87:2583–2588
- Magato A, Bueno V, Merino N (2013) Safety evaluation of *Morinda citrifolia* (noni) leaves extract: assessment of genotoxicity, oral short term and subchronic toxicity. *J Intercut Ethnopharmacol* 2:15–22
- Deng S, West B, Jensen C (2010) A quantitative comparison of phytochemical components in global noni fruits and their commercial products. *Food Chem* 122:267–270
- Muhammad Nadzri N, Abdul A, Sukari M, et al. (2013) Inclusion complex of zerumbone with hydroxypropyl-β-cyclodextrin induces apoptosis in liver hepatocellular HepG2 cells via caspase 8/BID cleavage switch and modulating BCL2/Bax ratio. *Evidence-Based Complementary and Alternative Medicine*, vol. 16
- Lu Z, Song Q, Jiang S, Wang W (2009) Identification of ATP synthase beta subunit (ATPB) on the cell surface as a non-small cell lung cancer (NSCLC) associated antigen. *BMC Cancer* 9:16
- Kurai J, Chikumi H, Hashimoto K et al (2007) Antibody-dependent cellular cytotoxicity mediated by cetuximab against lung cancer cell lines. *Clin Cancer Res* 13:1552–1561
- Lim S, Goh Y, Mustapha N, Rahman HS, Othman H, AbuBakar N, Mohamed S (2016) *Morinda citrifolia* edible leaves extract enhanced immune response against lung cancer. *Food Funct*. doi:10.1039/C5FO01475A

22. Liu X, Zhang L, Fu X et al (2001) Effect of scopoletin on PC3 cell proliferation and apoptosis. *Acta Pharmacol Sin* 22:929–933
23. Kim E, Kwon K, Shin B et al (2005) Scopoletin induces apoptosis in human promyeloleukemic cells, accompanied by activations of nuclear factor κ B and caspase-3. *Life Sci* 77:824–836
24. Saha A, Kuzuhara T, Echigo N et al (2010) New role of (–)-epicatechin in enhancing the induction of growth inhibition and apoptosis in human lung cancer cells by curcumin. *Cancer Prev Res* 3:953–962
25. Babich H, Krupka ME, Nissim HA, Zuckerbraun HL (2005) Differential in vitro cytotoxicity of (–)-epicatechin gallate (ECG) to cancer and normal cells from the human oral cavity. *Toxicol In Vitro* 19:231–242
26. Choudhury D, Das A, Bhattacharya A, Chakrabarti G (2010) Aqueous extract of ginger shows antiproliferative activity through disruption of microtubule network of cancer cells. *Food Chem Toxicol* 48:2872–2880
27. Mohan S, Bustamam A, Ibrahim S, et al. (2011) In vitro ultramorphological assessment of apoptosis on CEMss induced by linoleic acid-rich fraction from typhonium flagelliforme tuber. *Evidence-Based Complementary and alternative medicine*, vol. 12
28. Pao W, Chmielecki J (2010) Rational, biologically based treatment of EGFR-mutant non-small-cell lung cancer. *Nat Rev Cancer* 10:760–774
29. Brugger W, Triller N, Blasinska-Morawiec M et al (2011) Prospective molecular marker analyses of EGFR and KRAS from a randomized, placebo-controlled study of erlotinib maintenance therapy in advanced non-small-cell lung cancer. *J Clin Oncol* 29:4113–4120
30. Kung Y, Lin C, Liaw S et al (2011) Effects of erlotinib on pulmonary function and airway remodeling after sensitization and repeated allergen challenge in Brown-Norway rats. *Respir Physiol Neurobiol* 175:349–356
31. Lontas A, Yeger H (2004) Curcumin and resveratrol induce apoptosis and nuclear translocation and activation of p53 in human neuroblastoma. *Anticancer Res* 24:987–998
32. Fischer B, Coelho D, Dufour P et al (2003) Caspase 8-mediated cleavage of the pro-apoptotic BCL-2 family member BID in p53-dependent apoptosis. *Biochem Biophys Res Commun* 306:516–522
33. Javid J, Mir A, Ahamad I et al (2012) Impact of MDM2 SNP309T>G Polymorphism: increased risk of developing non small cell lung cancer and poor prognosis in Indian patients. *J Cancer Sci Ther* 04:341–346
34. Mita A, Mita M, Nawrocki S, Giles F (2008) Survivin: key regulator of mitosis and apoptosis and novel target for cancer therapeutics. *Clin Cancer Res* 14:5000–5005
35. Kren L, Brazdil J, Hermanova M et al (2004) Prognostic significance of anti-apoptosis proteins survivin and bcl-2 in non-small cell lung carcinomas: a clinicopathologic study of 102 cases. *Appl Immunohistochem Mol Morphol* 12:44–49
36. Zhao M, Gao F, Wang J et al (2011) JAK2/STAT3 signaling pathway activation mediates tumor angiogenesis by upregulation of VEGF and bFGF in non-small-cell lung cancer. *Lung Cancer* 73:366–374
37. Bhattacharya S, Ray R, Johnson L (2005) STAT3-mediated transcription of Bcl-2, Mcl-1 and c-IAP2 prevents apoptosis in polyamine-depleted cells. *Biochem J* 392:335–344
38. Niu G, Wright K, Ma Y et al (2005) Role of Stat3 in regulating p53 expression and function. *Mol Cell Biol* 25:7432–7440
39. Flowers L (2013) Targeting JAK-STAT signal transduction pathways in human carcinomas. *Int J Biosci* 3:241–250
40. Patel K, Ferrucci L, Ershler W et al (2009) Red blood cell distribution width and the risk of death in middle-aged and older adults. *Arch Intern Med* 169:515–523
41. Baicus C, Caraiola S, Rimbas M et al (2011) Utility of routine hematological and inflammation parameters for the diagnosis of cancer in involuntary weight loss. *J Investig Med* 59:951–955
42. Opal S, Depalo V (2000) Anti-inflammatory cytokines. *CHEST J* 117:1162–1172
43. Beppu M, Ikebe T, Shirasuna K (2002) The inhibitory effects of immunosuppressive factors, dexamethasone and interleukin-4, on NF- κ B-mediated protease production by oral cancer. *Biochim Biophys Acta* 1586:11–22
44. Kalluri R, Zeisberg M (2006) Fibroblasts in cancer. *Nat Rev Cancer* 6:392–401
45. Giacomelli L, Gianni W, Belfiore C et al (2003) Persistence of epidermal growth factor receptor and interleukin 10 in blood of colorectal cancer patients after surgery identifies patients with high risk to relapse. *Clin Cancer Res* 9:2678–2682
46. Mocellin S, Marincola F, Young H (2005) Interleukin-10 and the immune response against cancer: a counterpoint. *J Leukoc Biol* 78:1043–1051
47. Segal B, Glass D, Shevach E (2002) Cutting edge: IL-10-producing CD4+ T cells mediate tumor rejection. *J Immunol* 168:1–4
48. Mueller M, Hobiger S, Jungbauer A (2010) Anti-inflammatory activity of extracts from fruits, herbs and spices. *Food Chem* 122:987–996
49. De Bosscher K, Haegeman G, Elewaut D (2010) Targeting inflammation using selective glucocorticoid receptor modulators. *Curr Opin Pharmacol* 10:497–504
50. Theriault A, Wang Q, Van Iderstine S et al (2000) Modulation of hepatic lipoprotein synthesis and secretion by taxifolin, a plant flavonoid. *J Lipid Res* 41:1969–1979
51. Shaw C, Chen C, Hsu C et al (2003) Antioxidant properties of scopoletin isolated from *Sinomonium acutum*. *Phyther Res* 17:823–825
52. Shah Z, Li R, Ahmad A et al (2010) The flavanol (–)-epicatechin prevents stroke damage through the Nrf2/HO1 pathway. *J Cereb Blood Flow Metab* 30:1951–1961